Copyright © 2007 by ABCM

NUMERICAL AND EXPERIMENTAL ANALISYS OF INDENTATION ON A HYPERELASTIC CIRCULAR MEMBRANE

Djenane C. Pamplona djenane@civ.puc-rio.br
Stefane X. Lopes srx.lopes@uol.com.br
Hans I. Weber *hans@mec.puc-rio.br*
Guilherme Rodrigues Sampaio guirsp@hotmail.com
Pontifical Catholic University, PUC-Rio, Department of Civil Engineering
Rua Marquês de. São Vicente, 225 - 22453-900, Rio de Janeiro - Brazil

Abstract. *We examine the problem of indentation of an isotropic hyperelastic membrane by a rigid indenter in the shape of a right circular cylinder with different caps. The contact between the membrane and the metal tube is assumed frictionless. The equilibrium equations are obtained through the Principle of Stationary Potencial Energy. Our basic assumption is that the constitutive response of the membrane is characterized by a strain-energy function, which can be Neo-Hookean, Mooney Rivilin. A parametric study comparing the behavior and the stresses for different geometries for both constitutve equations is performed. To validate the numerical model, an experimental procedure is done. To do the experimental study an aparatus was buildt: a circular ring, where the membrane is pluged, is fixed in a certain position, while a motor drives a mechanism that linearly displaces an indenter with a given speed. Attached to the indenter is a force gage and a LVDT to measure the displacement. Two mirrors make it possible to observe de deformation of the membrane in two planes. The agreement of results between experimental and numerical analysis is rather encouraging.*
Keywords*: indentation, membrane, hiperelastic material*

1. INTRODUCTION

The penetration in membranes is a puzzling subject and its rupture by cavitation is very little studied. The possibility of rupture of the membrane requires special care in a great number of industrial processes. Its effective control or prevention becomes necessary for the protection of professionals of the medical area who use protective gloves and for a number of functions. The process of indentation of a membrane for rigid cylindrical objects is a classic example of the theory of unilateral restrictions, presented recently by Nadler (2006) and Steigmann (2007). Indentation of membranes has been subject of some recent articles Gianakoupolus (2006), Yan (2007) and Sampati (2006), but there is lack of experimental studies to testify the theoretical formulations that model the membrane behavior.

This research presents the numerical, analytical and experimental behavior of a circular flat membrane subjected to the transversal puncture by a cylindrical circular indenter. The material of the membrane is considered as homogenous, isotropic and hiperelastic, and is modeled as being of the Neo-Hookean type. The equilibrium equations and boundary conditions were obtained through the Principle of Stationary Potential Energy.

This is the first step of a project that will consider in its continuity the penetration of the indenter and cavitation. The study, reported in this paper, stops as the tangent to the lateral surface of the membrane at the external contact point becomes vertical. Only after this limit the penetration begins.

2. NUMERICAL FORMULATION

It is studied the behavior of a homogeneous flat circular membrane of radius R_2, under the action of cylindrical indenter with radius R_1 acting transversally in the center of the membrane. The membrane in question is considered constituted of a homogeneous, isotropic and incompressible material, behaving in a way that it can be considered made of a Neo-Hookean material. The problem is divided in two steps. In the first step the membrane, of uniform thickness *h*, deforms itself out of its plane taking the form of a trunk of cone closed in the superior part, R_1 and R_2 being the upper and lower radius, respectively, Fig. 1. This process continues until the superior part of the cone trunk arrives at an altitude limit, Z_1^*. In this moment the tangent to the curvilinear membrane surface is vertical. After this, if the action of the indenter proceeds, the penetration process starts when part of the membrane takes the form of the lateral surface of the indenter. Only the indentation is being considered in this paper. The contact at this first step is considered frictionless.

Despite the equations, that describe this type of problem, to be highly not linear, being solved only through numerical methods like finite methods of numerical integration (which transform the boundary value problem into a initial value problem), sometimes it is possible to develop an analytical formulation.

The independent variable is the radius of the undeformed membrane $0 < \rho < R_2$.

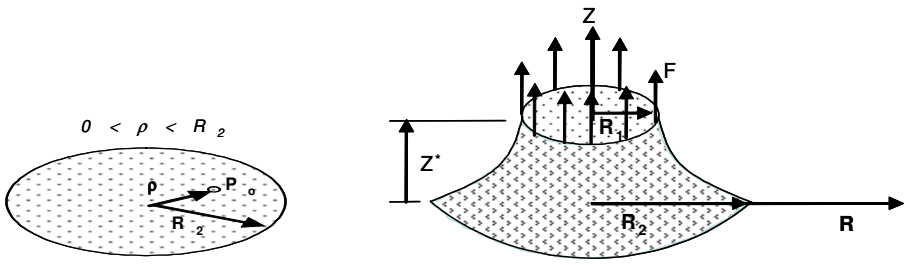

Figure 1. Membrane in the configurations (a) undeformed and (b) deformed.

To model the problem, the undeformed membrane was divided in two regions, which were studied independently along the two following stages. The inner region of radius *b* will cover the top of the trunk of cone (stage 1); the outer region will result in the spatial deformed membrane:

- **Stage 1** – Considers the flat superior part of the trunk of cone. $0 < \rho < b$, where *b* is the intermediary undeformed radius between the two stages, $0 < R(\rho) < R_1 \ and \ Z(\rho) = 0$.
- **Stage 2** – Indentation: the indenter stretches the other region of the undeformed flat membrane ($b < \rho < R_2$) out of its plane, until an imposed vertical displacement Z_1; in this way, $Z(b) = Z_1, \ \ Z(R_2) = 0.$

.

The mathematical modeling of the problem uses the formulation of continuum mechanics for finite deformations, as considered by Green and Adkins (1970). To assemble the two stages together a compatibility equation is considered.

2.1 First stage:

In this stage the plane deformation of a region of radius ***b*** in this own plane is considered, Fig. 2.

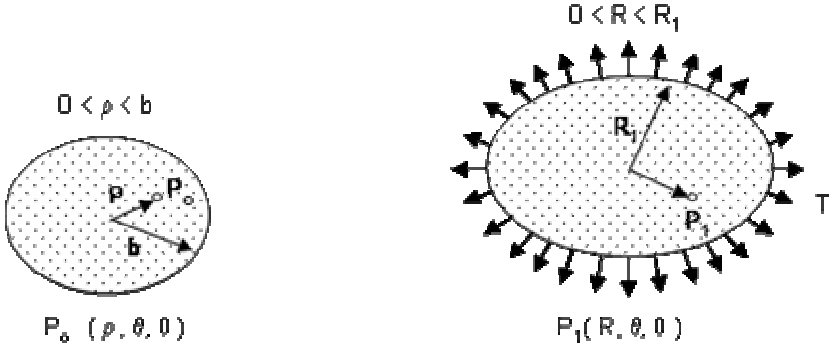

Figure 2. Stage 1: Plane deformation of part of the membrane, (a) undeformed $0 < \rho < b$ e (b) deformed $0 < R(\rho) < R_1$ and. $Z(\rho) = 0.$

The principal extensions λ_1, λ_2 and λ_3 , for the incompressible material, are:

$$\lambda_1 = R', \quad \lambda_2 = \frac{R}{\rho}$$

$$\lambda = \lambda_3 = \frac{h}{H} = \sqrt{\frac{\rho^2}{R'^2 R^2}} \tag{1}$$

Where: *h* and *H* are the undeformed and deformed thickness and $(\ )' = \frac{d(\ )}{d\rho}$.

In this way the first strain invariant I_1, is:

$$I_1 = R'^2 + \frac{R^2}{\rho^2} + \lambda^2 \tag{2}$$

The potential energy, π, by definition, is the difference between the elastic energy of deformation, *E,* and the work, τ , done by the external forces*, T:*

$$\pi = E - \tau \tag{3}$$

The elastic energy of deformation*, E,* is obtained by the integration, over the undeformed volume*, V*, of the function density of energy of deformation, *W*, which corresponds to the elastic potential measured by unit of undeformed volume.

$$E = \int_V W \, dV \tag{4}$$

Considering the incompressibility of the material, the function density of energy of deformation depends only on the first invariant I_1.

Neo–Hookean $W = C_1(I_1 - 3)$ with $C1=0.359628$ MPa.

The work, τ , resulting from the action of the external force*, T*, is:

$$\tau = 2\pi T \int [R' - 1] d\rho \tag{5}$$

Using Eq. 2 it is possible to obtain the Equilibrium equations and boundary conditions for this stage.

$$\rho h W_R - [\rho h W_{R'}]' = 0 \tag{6}$$

$$R(0) = 0 \quad and \quad R(b) = R_1$$

where: $W_{(\,)} = \dfrac{\partial W}{\partial (\,)}$.

2.2 Second stage:

This stage considers the out of plane deformation of a flat circular annular membrane, $b < \rho < R_2$, until a prescribed vertical displacement Z_1^*, Fig. 2.

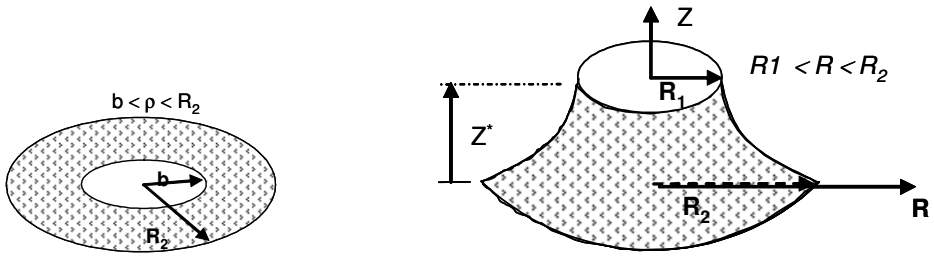

Figure 3. Stage 2. Membrane: (a) undeformed, $b < \rho < R_2$ e (b) deformed $R_1 < R < R_2$,
$R(b) = R_1, R(R_2) = R_2 \quad and \quad 0 \le Z(\rho) \le Z_1^*$.

The principal extensions λ_1, λ_2 and λ_3 are:

$$\lambda_1 = \sqrt{R'^2 + Z'^2} \quad \lambda_2 = \frac{R}{\rho} \qquad and \qquad \lambda_3 = \frac{1}{\lambda_1 \lambda_2} \tag{7}$$

The first strain invariant of deformation, I_1, is:

$$I_1 = \sqrt{R'^2 + Z'^2} + \frac{R^2}{\rho^2} + \lambda^2 \tag{8}$$

The work, τ, resulting from the action of the external force, F, is:

$$\tau = -F \int Z' \, d\rho \tag{9}$$

Using Eq. 2 and Eq. 8 it is possible to obtain the Equilibrium Equations and boundary conditions for this stage

$$\begin{aligned} &\rho h W_R - \left[\rho h W_{R'}\right]' = 0 \\ &0 - \left[2\pi\rho h W_{R'} + F\right]' = 0 \\ &R(c) = R_1; \quad 2\pi\rho h W_{Z'} + F\,|_{\rho=c} = 0 \\ &R(R_2) = R_2; \quad Z(c) = Z_1 \end{aligned} \tag{10}$$

3. EXPERIMENTAL MODEL

To measure the deformed membrane in three dimensions, an apparatus was build using a pair of mirrors fixed to a table, making possible the visualization of the sides of the membrane. In the central part of the mirror assembly the undeformed membrane is fixed through a circular ring on the table. The indenter is heaved with the help of a mechanical car jack driven by a speed controlled DC motor from a wiper. A 100 N load cell is mounted between the jack and the indenter and, its displacement is obtained with the help of a 30 cm LVDT (linear variable displacement transducer), Fig. 4.

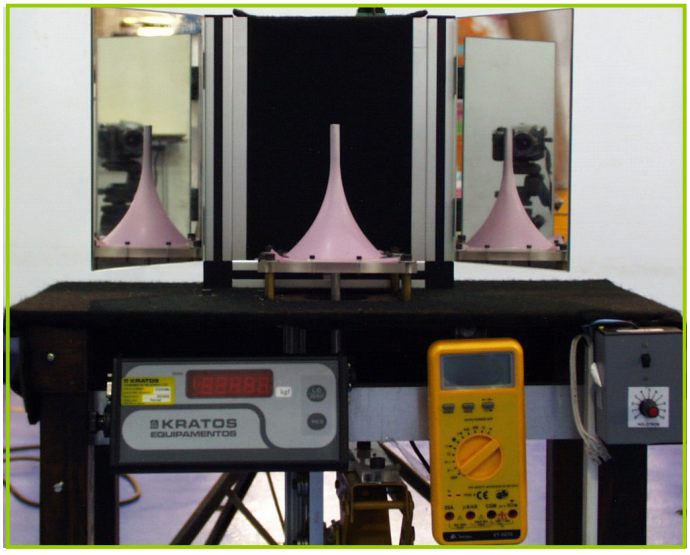

Figure 4` - Experimental apparatus.

4. RESULTS

4.1. Analytical results

Since the material is Neo-Hookean and there are large deformations the following assumption is considered:

$$\frac{1}{\lambda_1^4\lambda_2^2} \langle\langle 1 \quad and \quad \frac{1}{\lambda_2^4\lambda_1^2} \langle\langle 1 \tag{11}$$

In this way, using the equation of equilibrium and boundary conditions Eq. 6 with Eq. 1 (for stage 1), Eq. 10 with Eq. 8, (for stage 2); it is possible to find a closed form solution.

For the Stage 1, $0 \le \rho \le b$:

$$R(\rho) = \frac{R_1}{b}\rho \tag{12}$$

For the Stage 2; $b < \rho < R_2$:

$$R = D\rho + \frac{E}{\rho} \; where: D = \frac{R_2^2 - R_1 b}{R_2^2 - b^2}; E = \frac{R_2^2 b(R_1 - b)}{R_2^2 - b^2}$$

$$Z = -\frac{Z_1^*}{ln\left(\frac{R_2}{b}\right)} ln\left(\frac{\rho}{b}\right) \tag{13}$$

Considering the following compatibility equation one gets the solution Z_1

$$\lambda_3^{stage1}(b) = \lambda_3^{stage2}(b)$$

$$Z_1 = b\,ln\left(\frac{R_2}{b}\right)\sqrt{\left(\frac{R_1}{b}\right)^2 - \left(R'(b)\right)^2} \tag{14}$$

In Fig. 5 it is possible to observe the analytical solution for the stresses at a maximum vertical displacement Z^*=14 mm. After this point, the penetration begins and $R'(b)$ =0. In Fig. 6 it can be seen how the stresses in both directions behave for different vertical displacements Z^*.

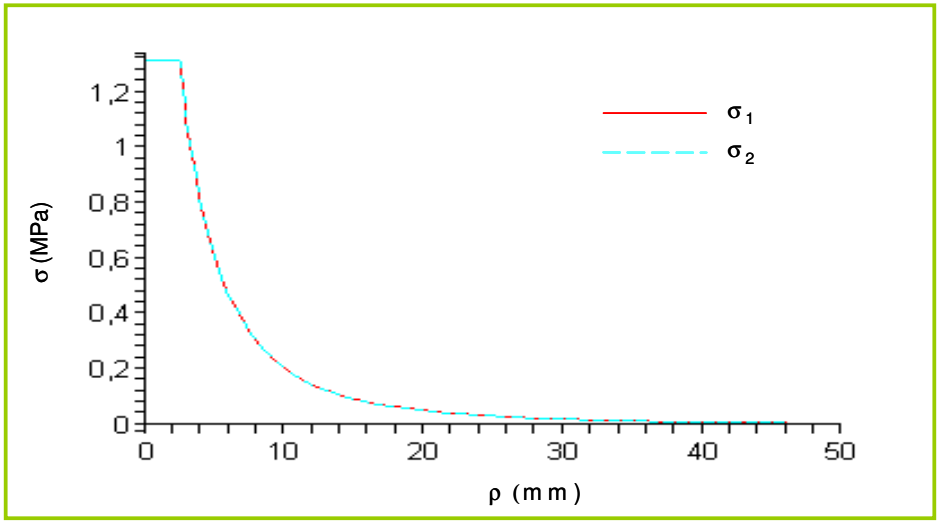

Figure 5` Meridional (σ_1) and Azimuthal (σ_2) stresses with Z*=14 mm.

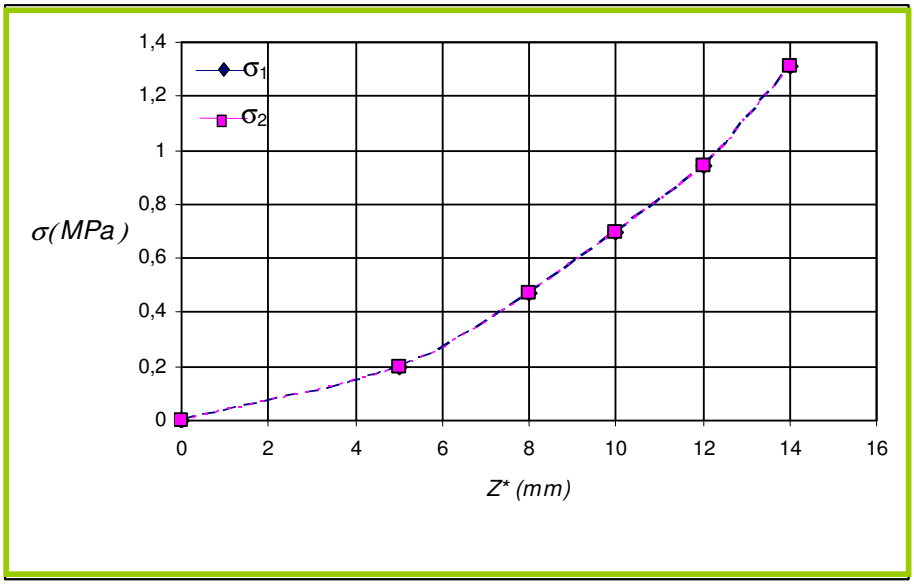

Figure 6. Variation of the Meridional (σ_1) and Azimuthal (σ_2) stresses with Z for Z*=14.0mm.

4.2. Numerical results

The numerical solution was done using the software of symbolic algebra Maple©, assembling a program to solve the equilibrium equations of the problem. To accomplish the inclusion of the boundary conditions in a suitable way it was necessary to use the shooting method coupled with the Newton Raphson Method. Since the problem is highly nonlinear the obtained analytical solutions were of fundamental importance to make the first guess of the boundary conditions.

In Fig. 7 and Fig. 8 it is possible to observe the numerical solutions for the stresses at Z*=14.0 mm and at the maximum vertical displacement Z*=27.9 mm, respectively, after this the penetration starts.

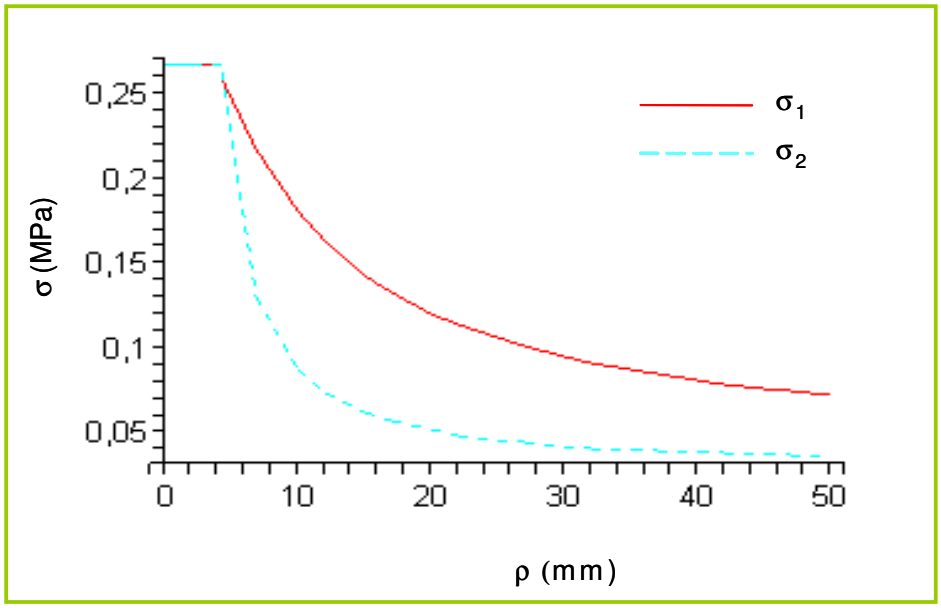

Figure 7. Meridional (σ_1) and Azimuthal (σ_2) stresses with Z*=14 mm.

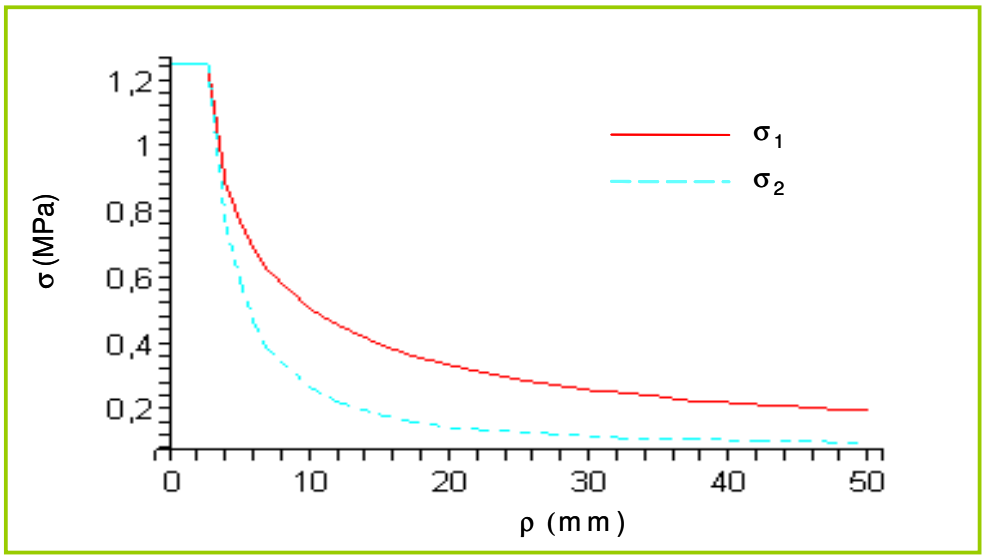

Figure 8. Meridional (σ_1) and Azimuthal (σ_2) stresses with Z*=27.9 mm.

4.3. Experimental results

Using the apparatus of Fig. 4, a rubber like membrane circular membrane, *Dental Dam* 5'' x 5'', with radius R_2=51mm and thickness h=0.186mm was deformed several times by a circular cylindrical indenter of radius R_1=4.7mm, as seen in Fig. 9 and 10.

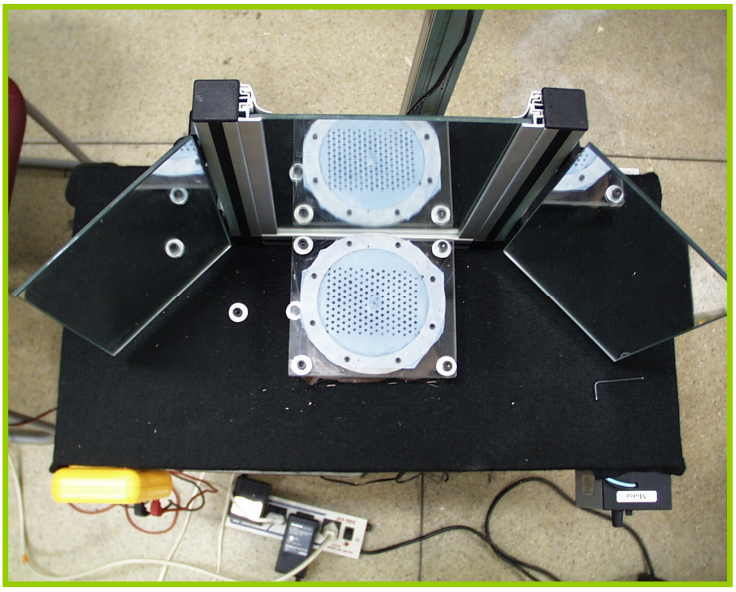

Figure 9. Upper view of the membrane in the apparatus.

In Fig. 10 it is possible to observe the deformed membrane during loading and unloading. The relation between the applied force in Newton and the measured vertical displacements of the membrane is seen in Fig. 11. This behavior is dependent of the velocity of the loading. To avoid viscoelastic effects maximum displacement of the indenter is attained in a quite short time period.

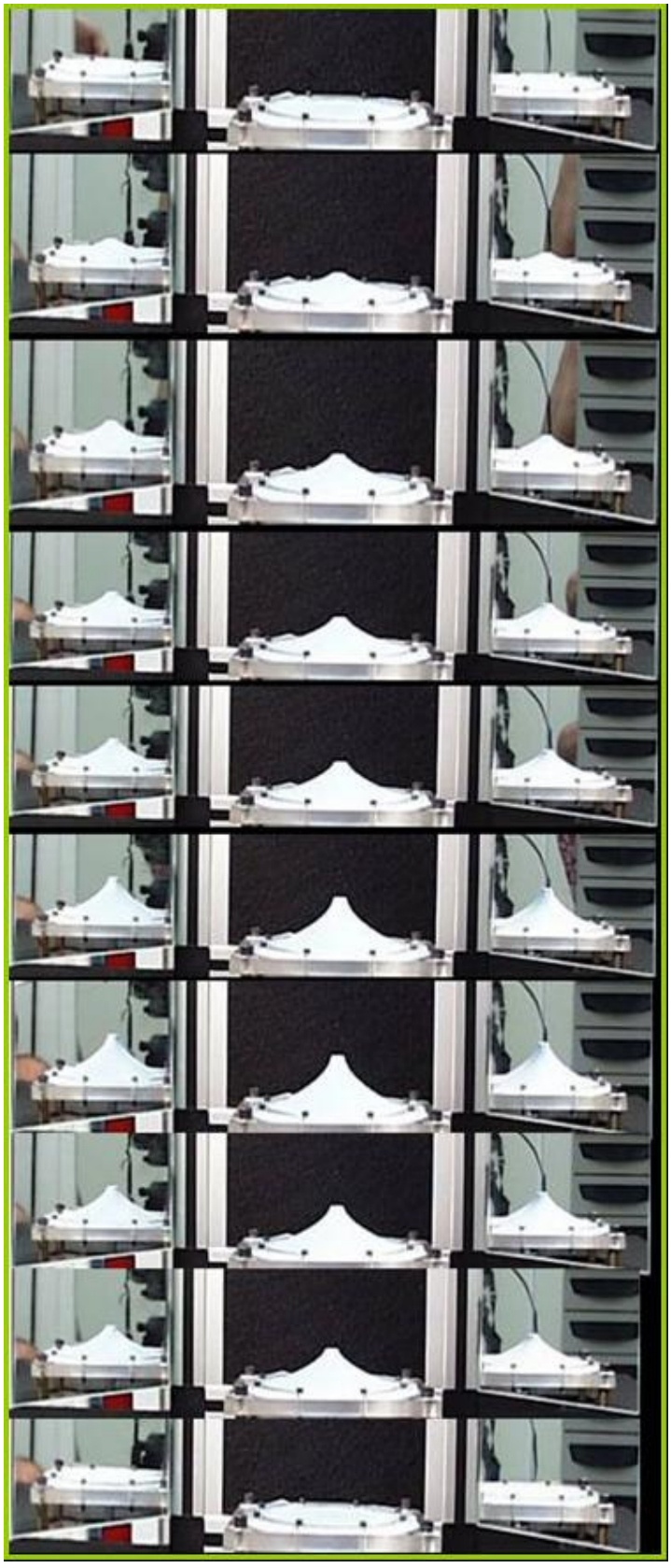

Figure 10. Loading and unloading of the membrane.

Figure 11. Displacement Z (cm) in relation with force F (N).

4.3. Comparison between experimental, analytical and numerical results.

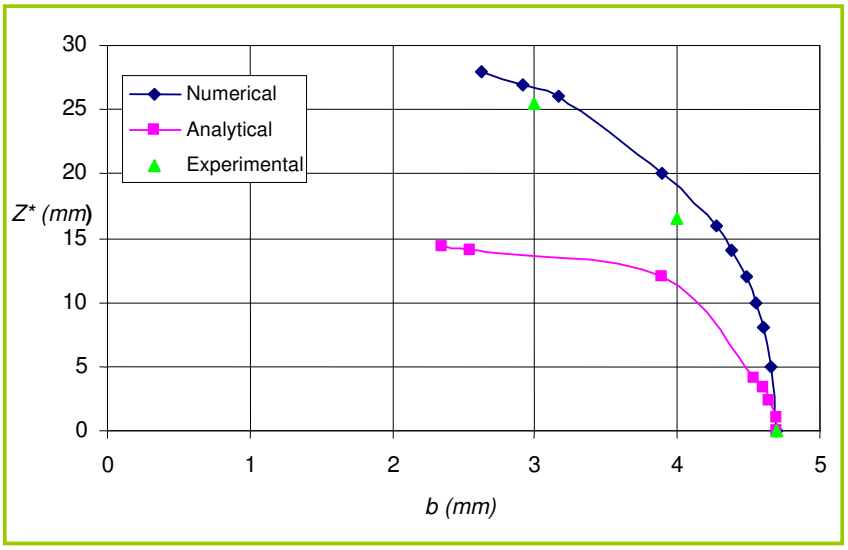

Figure 12. Relation of vertical displacement Z*(mm) with b (mm), the intermediary undeformed radius between the two stages, for the three cases: experimental, analytical and numerical.

Figure 13 shows the analytical and the numerical stresses related with the prescribed displacement Z_1^*. It can be seen that for the same prescribed vertical displacement Z_1^*, the maximum stress obtained in the analytical model is almost twice of the obtained with the numerical model. Although, both models achieve the same maximum stress, when R'=0, that is the maximum displacement before starting the penetration.

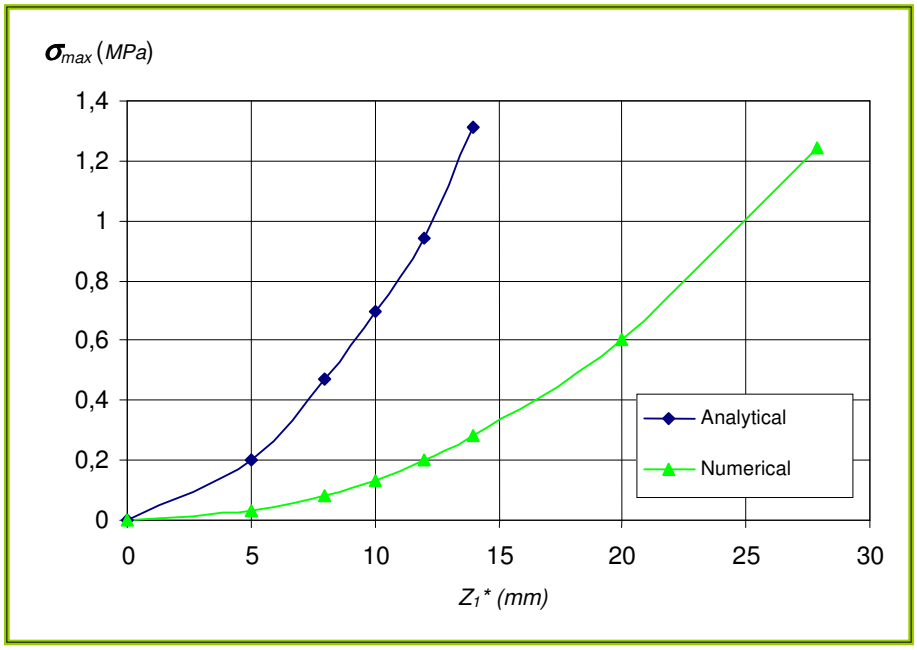

Figure 13. Relation of Z_1*(mm) with b (mm), the intermediary undeformed radius between the two stages, for the tree results.

5 – CONCLUSIONS

The assumption of Eq. [11] used to obtain the analytical solution considering very large strains is not good for this part of the problem, because we are neglecting at some values of the coordinate ρ, 0.3 in the presence of 1. Even though the analytical solutions are of much importance to give a first approximation for the boundaries conditions to be used the shooting method.

The stresses obtained analytically are twice the ones obtained numerically, although both models achieve the same maximum stress, when $R' = 0$, that is the maximum displacement before the start of penetration.

The intermediary undeformed radius between the two stages, b, obtained numerically is half the one obtained analytically for the same prescribed vertical displacement, although the comparison between numerical and experimental behavior is rather good.

As it was said before this is a first step to be completed before investigating penetration and cavitation, the results obtained here are quite encouraging.

6. ACKNOWLEDGEMENTS

We are grateful to CNPq and FAPERJ for their financial support through the grants and also to Professor David Steigmann for the idea of the present research.

7. REFERENCES

Gianakoupolus A.E., 2006, "Elastic and Viscoelastic Indentation of Flat Surfaces by Pyramid Indenters", *J. Mech. and Phys. of Solids*, Vol. 54, pp 1305-1332.

Green A.E. and Adkins J.E., 1970, "Large Elastic Deformations", Clarendon Press, Oxford UK, 324p.

Nadler B and Steigmann D, 2006, "Modeling Indentation, Penetration and Cavitation of elastic Membranes", *J.Mech. and Phis of Solids*, Vol. 54, pp 2005-2029.

Sampati K. et all, 2006, "Numerical Analysis of Spherical Indentation of Thin Hard Films", *Int. J. Solids and Structures*, Vol. 43, pp 6180, 6193.

Sergici O. et all ,"Adhesion and Contact of Spherical Indenter with a Layered Elastic Half-space", *J. Mech. and Phys of Solids*, Vol. 54, pp 272-297, 2006.

Steigmann D., 2007, "Puncturing a Thin Elastic Sheet", *Int. J. Non-linear Mechanics*, to appear.

Yan W. et all, 2007, "Analysis of Spherical Indentation of Super Elastic Shape Memory Alloys", *Int. J. Solids and Structures*, Vol. 44, pp 1-17.